First Principles Phase Diagram Calculations for the System NaCl-KCl: the role of excess vibrational entropy.

B.P. Burton[1] and A. van de Walle[2]

[1]*Materials Science and Engineering Laboratory,*

Ceramics Division National Institute of Standards and Technology,

Gaithersburg, MD 20899, USA; benjamin.burton@nist.gov,

Phone: 301-975-6053, FAX: 301-975-5334.

[2]*Materials Science and Engineering Department,*

Northwestern University 2225 North Campus Dr.,

Evanston, IL 60208, USA; avdw@northwestern.edu

Abstract

First principles phase diagram calculations were performed for the system NaCl-KCl. Planewave pseudopotential calculations of formation energies were used as a basis for fitting cluster expansion Hamiltonians, both with- and without an approximation for the excess vibrational entropy (S_{VIB}). Including S_{VIB} dramatically improves the agreement between calculated and experimental phase diagrams: experimentally, the consolute point is $\{X_C = 0.348, T_C = 765K\}_{Exp}$; without S_{VIB}, it is $\{X_C = 0.46, T_C \approx 1630K\}_{Calc}$; with S_{VIB}, it is $\{X_C = 0.43, T_C \approx 930K\}_{Calc}$.

Key words: NaCl-KCl; First Principles; Phase diagram calculation; Excess vibrational entropy; insulator; ionic system.

Submitted to **Chemical Geology** 1/05.

I. INTRODUCTION

In roughly the last decade, there have been many theoretical and experimental investigations of the effects of excess vibrational entropy, S_{VIB}, on phase stabilities of intermetallics and alloys: e.g. Garbulsky and Ceder (1994) and (1996); Silverman et al. (1995a, 1995b); Tepesch et al. (1996); van de Walle et al. (1998); Ozolins et al. (1998); Ravelo et al. (1998); van de Walle and Ceder (2000); Asta and Ozolins (2001); Wolverton and Ozolins (2001); van de Walle and Ceder (2002a); and Wu et al. (2003); Anthony et al. (1993) and (1994); Fultz et al. (1995a) and (1995b); Nagel et al. (1997); Frase et al. (1998); Bogdanoff et al. (1999); Robertson et al. (1999); Manley et al. (2002); and Delaire et al. (2004). For a recent review, see van de Walle and Ceder (2002a) which tabulates 19 systems that have been modeled theoretically and 16 that have been studied experimentally.

The vast majority of studies focus on the stabilities of intermetallic compounds, and publications on ionic insulating systems are limited to one theoretical study of the MgO-CaO system (Tepesch et al., 1996). To further investigate vibrational effects in ionic insulating systems, a first-principles phase diagram (FPPD) calculation was performed for the NaCl-KCl quasibinary system, which included the effects of both configurational and vibrational disorder. The FPPD computational approach allows a direct assessment of the effects of lattice vibrations on phase stability by comparing the phase diagrams that were calculated with and without the inclusion of vibrational effects.

This work makes two main contributions: first, because the NaCl-KCl phase diagram is well characterized experimentally (Nacken, 1918; Barrett and Wallace, 1954; Bunk and Tichelaar, 1953 and Walker et al. 2005), and well fit to regular-type solution models (Thompson and Waldbaum 1969 and Walker et al., 2005) it is an additional benchmark for the accuracy of the recently introduced "bond-length-dependent transferable force constants" approach for calculating lattice dynamics (van de Walle and Ceder (2002a), Wu et al., 2003); second, NaCl-KCl is an ionic system in which the effects of lattice vibrations are predicted to be exceptionally large, e.g. when vibrational entropy S_{VIB} is included, we find that the

calculated consolute temperature, T_C, is reduced by $\approx 54\%$ according to the formula:

$$\%\Delta T_C = 100\frac{2(T_C - T_C^{VIB})}{(T_C + T_C^{VIB})} \tag{1.1}$$

where T_C^{VIB} and T_C are values for T_C that were calculated with and without S_{VIB}, respectively. This is in sharp contrast with previous results of Tepesch et al. (1996), who studied the isostructural MgO-CaO system, and Silverman et al. (1995a, 1995b) who studied the semiconductor, miscibility-gap system, GaP-InP: Tepesch et al. (1996) report a reduction in T_C of less than 10% while Silverman et al. (1995a, 1995b) report $\%\Delta T_C \approx 3\%$ for GaP-InP.

II. METHODOLOGY

A. Total Energy Calculations

Formation energies, ΔE_f (see Fig. 1) were calculated for NaCl, KCl, and many $Na_mK_nCl_{(m+n)}$ supercells. All calculations were performed with the Vienna *ab initio* simulation program (VASP; Kresse et al, 1993) using ultrasoft Vanderbilt type plane-wave pseudopotentials (Vanderbilt 1990) with the generalized gradient approximation (GGA) for exchange and correlation energies. Electronic degrees of freedom were optimized with a conjugate gradient algorithm, and both cell constant and ionic positions were fully relaxed. Valence electron configurations for the pseudopotentials are: Na $2p^6 3s^1$; K $3p^6 4s^1$; Cl $3s^2 3p^5$. Total energy calculations were converged with respect to k-point meshes, and an energy cutoff of 400 eV was used, in the "high precision" option which guarantees that *absolute* energies are converged to within a few meV (a few tenths of a kJ/mol of exchangeable cations; Na^+ or K^+).

B. Cluster Expansion construction

The cluster expansion (CE; Sanchez et al., 1984), is a compact representation of the alloy's configurational total energy. In the quasibinary NaCl-KCl system, the alloy configuration is described by pseudospin occupation variables σ_i, which take values $\sigma_i = -1$ when site-i is occupied by Na^+ and $\sigma_i = +1$ when site-i is occupied by K^+.

The CE parameterizes the configurational energy, per exchangeable cation, as a polynomial in pseudospin occupation variables:

$$E(\sigma) = \sum_{\ell} m_{\ell} J_{\ell} \left\langle \prod_{i \in \ell'} \sigma_i \right\rangle \tag{2.1}$$

where the cluster ℓ is defined as a set of lattice sites. The sum is taken over all clusters ℓ that are not symmetrically equivalent in the parent structure space group, and the average is taken over all clusters ℓ' that are symmetrically equivalent to ℓ. Coefficients J_{ℓ} are called effective cluster interactions (ECI), and the *multiplicity* of a cluster, m_{ℓ}, is the number of symmetrically equivalent clusters, divided by the number of cation sites. The ECI are obtained by fitting a set of FP calculated structure energies, $\{E_{Str}\}$. The resulting CE can be improved as necessary by increasing the number of clusters ℓ and/or the number of E_{Str} used in the fit.

Fitting was performed with the Alloy Theoretic Automated Toolkit (ATAT) (van de Walle, Asta and Ceder, 2002a; van de Walle and Ceder, 2002b; van de Walle and Asta, 2002) which automates most of the tasks associated with the construction of a CE Hamiltonian. A complete description of the algorithms underlying the code can be found in (van de Walle and Ceder, 2002b). The most important steps are: 1) Selecting which FP structural energies to calculate, which is done in a way that minimizes the statistical variance of the estimated ECI; 2) Automatically selecting which clusters to include in the expansion by minimizing the *cross-validation score*, CV:

$$(CV)^2 = \frac{1}{N} \sum_{Str=1}^{N} (E_{Str} - \hat{E}_{Str})^2 \tag{2.2}$$

where $E_1, \ldots E_N$ denote the structural energies calculated from FP and $\hat{E}_{Str}$ is the energy of structure Str *predicted* from a CE that was fit to the remaining $N-1$ energies. This criterion ensures that the chosen set of clusters maximizes the predictive power of the CE for any structure, whether or not it is included in the fit. This is an improvement relative to the standard mean square error criterion which only minimizes the error for structures that are included in the fit. The optimal number of clusters was found to be (10 pairs, nine triplets one 4-body; Table I), corresponding to a CV score of 0.068 eV.

In addition to the CV-criterion, ATAT also ensures that ground states predicted from the CE agree with the minimum energy structures for each composition, as calculated from FP. The code proceeds by iterative refinement, gradually increasing the number of clusters and the number of structures to provide the best possible fit based on the set $\{E_{Str}\}$ calculated so far.

C. Lattice Dynamics

The contribution of lattice vibrations to the alloy free energy were calculated using bond-length-dependent transferable force constants (van de Walle and Ceder, 2002a; Wu, Ceder and van de Walle, 2003), as implemented in the ATAT package. This method has the advantage of avoiding the computationally demanding task of performing full first-principles lattice dynamic analyses for each supercell configuration that is used to fit the cluster expansion. Instead, a much smaller database of first-principles calculations is typically sufficient for a FPPD calculation.

This method proceeds by parameterizing the bond-length-dependence of the stiffness for each type of nearest-neighbor chemical bond. This is achieved by calculating, ab initio, the reaction forces from various imposed atomic displacements away from their equilibrium positions, which is done only for a few high-symmetry ordered supercells over a range of lattice parameters. In the present work, only the two end member structures were considered, for 3 or 4 values of the lattice parameter, ranging from about 2.8 Å to about 3.2 Å (roughly corresponding to the equilibrium lattice parameters of NaCl and KCl, respectively). Due to the high-symmetry of these structures, two symmetrically distinct displacements are sufficient to determine all force constants. The parameters defining the bond-length-dependent transferable force constants are then obtained from a polynomial fit of the calculated forces as a function of bond length. As shown in Figure 2, a linear relationship was found to provide a reliable description of interactions in this system.

Once the bond-length-dependence of bond-stiffness is known, the nearest-neighbor interatomic force constants for any supercell configuration in the cluster expansion fit can be predicted from the relaxed bond lengths that are obtained from the VASP structure energy minimizations. A standard lattice dynamics based on a nearest-neighbor Born-von Kármán model (e.g. van de Walle and Ceder, 2002a; Maradudin, Montroll and Weiss, 1971) provides

the phonon density of states and, consequently, any thermodynamic property of interest, such as the vibrational contribution to the free energy for each supercell configuration.

Configuration dependence of the vibrational free energy is parametrized with a cluster expansion, in a similar manner as the energy at absolute zero, except that the resulting effective cluster interactions are now temperature-dependent. The alloy's thermodynamic properties are then calculated via conventional Monte-Carlo simulations of a lattice gas model using the temperature-dependent cluster expansion Hamiltonian.

III. RESULTS

A. Formation Energies

Calculated formation energies, ΔE_f, for 45 $Na_mK_nCl_{(m+n)}$ supercells are plotted in Fig. 1. Values for ΔE_f are normalized per mol of exchangeable Na^+ and K^+ ions:

$$\Delta E_f = (E_S - mE_{NaCl} - nE_{KCl})/(m+n) \tag{3.1}$$

Where E_S is the total energy of the supercell; E_{NaCl} is the energy/mol of NaCl; E_{KCl} is the energy/mol of KCl.

All supercell energies are positive which indicates a miscibility gap system.

B. Cell Volume

The VASP GGA results for end member cell volumes are listed in Table I. Differences between experimental and calculated values are less than 6%.

Figure 3 is a plot of normalized excess volumes as percentages: $\%\Delta V = 100(V - V_{Vegard})/V_{Vegard}$, where $V_{Vegard} = (1-X)V_{NaCl} + (X)V_{KCl}$. Experimental data from Barrett and Wallace (1954) □, are all greater than zero, with all $\Delta V_{EXP} \leq 0.4\%$. The large •-curve is for VASP-calculated supercells which, with only one exception, have $\%\Delta V = \pm 2\%$. A $T \to \infty$ calculation of $\%\Delta V(X)$ was performed, small-• curve, and it does not deviate significantly from Vegard's law. The ⧫-curve was calculated at 1100K which corresponds to the experimental value of 630C = 903K, in T/T_C units. Because of Na/K short-range clustering, this curve is in somewhat better agreement with experiment, but there is still a

significant discrepancy.

The results of FPPD calculations that were performed with (solid curve) and without (dashed curve) S_{VIB} are compared with the experimental data of Nacken (1918) Bunk and Tichelaar (1953) and Barrett and Wallace (1954). Including S_{VIB} clearly leads to dramatic improvement in the agreement between experiment and theory, but even with S_{VIB} included $T_C^{Calc} \approx 1.18 T_C^{EXP}$, and both with and without S_{VIB}, $X_C^{Calc} \approx 0.43$ is significantly greater than $X_C^{EXP} = 0.348$, Thompson and Waldbaum (1969). The experimental diagram exhibits significantly greater asymmetry than the calculated diagrams. Because the effective Hamiltonian that included S_{VIB} only has T-dependence in pair interactions, it naturally yields a more symmetric phase diagram; i.e. the T-dependent part of the Hamiltonian is strictly symmetric, so adding it to the T-independent part reduces the asymmetry. In light of these observations, it should be possible to further improve on the accuracy of our calculations by including T-dependent 3-body interactions, which will require considering a larger database of structures in the fit of the cluster expansion.

IV. DISCUSSION

The bond-length-dependent transferable force constants approach includes a set of approximations that beg some motivation and justification. Force constants associated with interactions ranging beyond nearest neighbors are typically not transferable from one structure to another, and therefore, are usually not included in this framework. Fortunately, quantities that are expressed in terms of sums over all vibrational modes, such as the vibrational free energy, are typically well-described with short-range spring models, unlike the phonon dispersion curves themselves (van de Walle and Ceder, 2002a ; Garbulsky and Ceder, 1996). When, as here, the focus is on phase stability rather than an exact description of phonon dispersion curves, this approximation is appropriate. It may be surprising that neglecting the long-range electrostatic interactions would yield a good approximation for the vibrational free energy, but because the Na^+ and K^+ ions have identical charges, purely electrostatic contributions to the force constants are expected to be nearly configuration-independent (apart from small shifts in atomic positions due to different ionic sizes). Most errors arising from this simplification should therefore cancel out in calculations of free energies of formation. Also, it is well known that to properly model phonon dispersions near the

gamma point of an ionic solid requires a special treatment of the interactions between the induced dipoles and the associated isotropic electric field via Born effective charges (Resta et al., 1993). While this effect is neglected in the present calculations, it is also known that long wavelength phonons make relatively small contributions to a solid solution's free energy of formation (Garbulsky and Ceder, 1996).

As noted in van de Walle and Ceder (2002a) and references therein, S_{VIB} is sometimes significant and sometimes vanishingly small. For example, FP calculations for Ni_3Al, van de Walle et al. (1998), indicate that S_{VIB} makes no significant contribution to the ordering energy. Similarly, as noted in the introduction, the results of Tepesch et al. (1996) suggest that it plays a very small role in MgO-CaO, a T_C-reduction of less than 10%; and Silverman et al. (1995a, 1995b) report a T_C-reduction of only 3% in GaP-InP. In contrast, the NaCl-KCl system is a case in which the effect of lattice vibrations is exceptionally large.

Three mechanisms that lead to significant S_{VIB} contributions to the free energies of solutions have been identified (Garbulsky and Ceder, 1994; Ackland, 1994; Althoff et al., (1997); van de Walle et al. (1998); Morgan et al. (2000); van de Walle and Ceder, 2002a) and it is of interest to identify the mechanisms at work in the NaCl-KCl system.

The "bond proportion" mechanism results from changes in an alloy's state of order that change the relative numbers of different types of chemical bonds. Because each bond has an intrinsic stiffness, this results in a change in the overall stiffness of the alloy and, consequently, a change in S_{VIB}. In the lattice dynamics calculations presented here, however, only first-nearest-neighbor force constants, for Na–Cl and K–Cl bonds are included, and the number of Na–Cl and K–Cl bond is a function of composition only, regardless of cation ordering. Therefore, the bond proportion mechanism cannot explain the results presented here.

The "volume" mechanism is a more likely candidate because NaCl-KCl does exhibit a positive excess volume of mixing, as seen in Fig. 3. S_{VIB} increases with increasing volume, which implies a positive entropy of mixing correlates with a positive excess volume of mixing, and a reduction in T_C. However, an excess volume of at most 0.2% (in our calculations) corresponds to an increase of at most $0.02k_B$ in the vibrational entropy, for plausible values of the Grüneisen parameter. Such a value is too small to entirely explain the large vibrational effect observed here.

The "size mismatch" mechanism is another plausible cause for the large S_{VIB} in NaCl-KCl. When ions of different size, (Na^+ K^+) mix in a crystalline solution, smaller Na^+ ions

are under tension, and larger K^+ are under compression, which shifts the vibrational density of states. The ionic radius ratios, Na^+/K^+=0.74 and Mg^{+2}/Ca^{+2}=0.72 (Shannon and Prewitt, 1969; Stobolov and Cohen, 2002) are very similar so it seems surprising that vibrational effects are large in NaCl-KCl and small in MgO-CaO, but size mismatch is only part of the story. The effects of bond-length changes on bond-stiffnesses must also be taken into account. Figure 5 compares the stiffnesses of bonds in NaCl-KCl with those in MgO-CaO as functions of composition. The composition-dependences of bond-stiffnesses are obtained under a series of simplifying assumptions designed to isolate the root of the differences in the magnitude of the vibrational effect:

1. The equilibrium volume is assumed linear in composition;

2. Atoms do not relax away from ideal crystallographic sites (so that volume uniquely determines bond lengths);

3. Bond lengths uniquely determine bond-stiffnesses, as shown in Figure 2 for NaCl-KCl (similar calculations were carried out for MgO-CaO but are not reported here for conciseness);

4. Only the bond-stiffness along the stretching direction is considered.

In both systems, one type of chemical bond reaches zero stiffness for some composition. Of course, this does not necessarily imply that the alloy is unstable at that point because the bending force constants (omitted in the graph) contribute to stabilize the solid. Nevertheless, the presence of a vanishing (or negative) force constant along the stretching direction indicates a relatively soft alloy with a large S_{VIB}. As seen in Figure 5, the Na-Cl bond-stiffness is positive in NaCl but goes through zero at $X_{KCL} \approx 0.55$, which indicates that soft Na-Cl bonds in the disordered alloy will increase S_{VIB}. In contrast, Mg-O bond-stiffness remains positive over most of the concentration range, and only crosses zero at a composition at which there are very few soft Mg-O bonds. Therefore, the disordered $Mg_{1-X}Ca_XO$ alloy is not significantly softened by Mg-O bonds. This important distinction appears to be at the root of the difference between the magnitude of vibrational effects in the NaCl-KCl and the MgO-CaO systems.

V. CONCLUSIONS

In the system NaCl-KCl, including S_{VIB} in the FPPD calculation dramatically improves the agreement between theory and experiment, but does not produce quantitative agreement with respect to either T_C or X_C. Note, that the improvement which is obtained by including S_{VIB} in the NaCl-KCl FPPD calculation yields agreement with experiment that is similar to that achieved for the systems $CaCO_3 - MgCO_3$ and $CaCO_3 - CdCO_3$, without including S_{VIB}, Burton and van de Walle (2003). Given the paucity of studies on ionic systems, and that both this study, and Tepesch et al. (1996) were of simple NaCl-structure solid solutions, it is premature to draw general conclusions about the benefits of including S_{VIB} in any particular FPPD calculation. In particular, results for solid solutions in more complex mineral structures, e.g. $Mg_2SiO_4 - Ca_2SiO_4$ or $CaCO_3 - MgCO_3$, in which cation ordering interacts with a more complex distribution of vibrational modes.

ACKNOWLEDGEMENTS

This work is supported by the U.S. National Science Foundation under program DMR-0080766, by the U.S. Department of Energy and the Air Force Office of Scientific Research under the MEANS program, grant no. F49620-01-1-0529.

VI. REFERENCES

Ackland, G.J., (1994) in *Alloy Modelling and Design*, edited by G. Stocks and P. Turchi (The Minerals, Metals and Materials Society, Pittsburg, PA), pp. 149.

Althoff, J. D., Morgan, D., de Fontaine, D., Asta, M., Foiles, S. M., and Johnson, D. D., (1997). Vibrational spectra in ordered and disordered Ni_3Al, Phys. Rev. B 56, R5705.

Anthony, L., Okamoto, J.K., and Fultz, B. (1993). Vibrational entropy of ordered and disordered Ni_3Al Phys. Rev. Lett. 70, 1128-1130.

Anthony, L., Nagel, L.J., Okamoto, J.K., and Fultz, B. (1994). Magnitude and Origin of the Difference in Vibrational Entropy between Ordered and Disordered Fe_3Al. Phys. Rev. Lett. 73, 3034-3037.

Asta, M. and Ozolins, V. (2001). Structural, vibrational, and thermodynamic properties of Al-Sc alloys and intermetallic compounds. Phys. Rev. *B64*, 094104-1-14.
Barrett, W.T. and Wallace, W.E. (1954). Studies of NaCl-KCl solid solutions. I. Heats of formation, lattice spacings, densities, Schottky defects and mutual solubilities. J. Amer. Chem. Soc. **76**, 366-369.

Bogdanoff, P.D. Fultz, B., and Rosenkranz, S., (1999). Vibrational entropy of $L1_2$ Cu_3Au measured by inelastic neutron scattering Phys. Rev. B 60, 3976-3981.

Bunk, A.J.H. and Tichelaar, G.W. (1953). Investigations in the system NaCl-KCl. Proc. Kon. Ned. Akad. Wetensch, **56**, 375-384.

Burton, B.P. and van de Walle, A., (2003). First Principles Based Calculations of the $CaCO_3$-$MgCO_3$ Subsolidus Phase Diagrams. Phys. Chem. Minerals 30, 88-97.
Delaire, O., Swan-Wood, T., and Fultz, B. (2004). Negative Entropy of Mixing for Vanadium-Platinum Solutions. Phys. Rev. Lett. 93, 185704 (2004).

Frase, H, Fultz, B. and Robertson, J.L. (1998). Phonons in nanocrystalline Ni_3Fe. Phys. Rev B57, 898-905.
Fultz, B., Anthony, L., Robertson, J.L. Nicklow, R.M. Spooner, S., and Mostoller, M. (1995a). Phonon modes and vibrational entropy of mixing in Fe-Cr. Phys. Rev. B 52, 3280-3285.

Fultz, B., Anthony, Nagel, L. J., Nicklow, and Spooner, S., (1995b). Phonon densities of states and vibrational entropies of ordered and disordered Ni_3Al. Phys. Rev. B 52, 3315-3321.

Garbulsky, G.D. and Ceder, G. (1994) Effect of lattice vibrations on the ordering tendencies in substitutional binary alloys. Phys. Rev. **B49**, 6327-6330.

Garbulsky, G.D. and Ceder, G. (1996). Contribution of the vibrational free energy to phase stability in substitutional alloys: Methods and trends. Phys. Rev. **B53**, 8993-9001.

Kresse, G. and Hafner, J., Ab initio molecular dynamics for liquid metals Phys. Rev. **B47**: 558-561 (1993); Kresse, G. Thesis, Technische Universität Wien (1993); Phys. Rev. **B49**: 14 251 (1994). Kresse, G. and Furthmüller, J. (1996) Efficiency of ab-initio total energy calculations for metals and semiconductors using a plane-wave basis set Comput. Mat. Sci. **6**: 15-50; Efficient iterative schemes for ab initio total-energy calculations using a plane-wave basis set Phys. Rev. **B54**: 11169 (1996); cf.
http://tph.tuwien.ac.at/ vasp/guide/vasp.html.

Manley, M.E., McQueeney, R.J., Fultz, B., Osborn, R., Kwei, G.H. and Bogdanoff, P.D. (2002). Vibrational and electronic entropy of beta -cerium and gamma -cerium measured by inelastic neutron scattering. Phys. Rev. B 65, 144111 (2002).

Maradudin A. A., Montroll, E. W. and Weiss, G. H., Theory of Lattice Dynamics in the Harmonic Approximation, Second Edition, Academic Press, New York (1971).
Morgan, D., van de Walle, A., Ceder, G., Althoff J. D. and de Fontaine, D., Modell. Simul. Mater. Sci. Eng. 8, 295 (2000).
Nacken, R. (1918). Über die Grenzen der Mischkristallbildung zwischen Kaliumchlorid und Natriumchlorid. Sitzungsber. Preuss. Akad. Wiss., Phys. Math. Kl. 192-200.

Nagel, L.J., Fultz, B., Robertson, J.L., and Spooner, S. (1997). Vibrational entropy and microstructural effects on the thermodynamics of partially disordered and ordered Ni_3V. Phys. Rev. B 55, 2903-2911.

Ozolins, V., Wolverton, C., and Zunger, Alex, (1998). First-principles theory of vibrational effects on the phase stability of Cu-Au compounds and alloys Phys. Rev. B 58, R5897-R5900.

Ravelo, R., Aguilar, J., Baskes, M., Angelo, J. E., Fultz, B., and Holian, B. L., (1998). Free energy and vibrational entropy difference between ordered and disordered Ni_3Al. Phys. Rev. B 57, 862-869.

Resta, R, Posternak, M. and Baldereschi, A. (1993) Towards a quantum theory of polarization in ferroelectrics: The case of $KNbO_3$. Phys. Rev. Lett. 70, 1010-1013

Robertson, J. L., Fultz, B., and Frase, H. N., (1999). Phonon contributions to the entropies of hP24 and fcc Co_3V. Phys. Rev. B 60, 9329-9334.

Sanchez, J.M., Ducastelle, F. and Gratias, D., (1984). Generalized cluster description of multicomponent systems. Physica **128A**, 334-350.

Shannon, R.D. and Prewitt, C. T. (1969). Effective ionic radii in oxides and fluorides. Acta Cryst. B25, 925-946.

Silverman, S. Zunger, A. Kalish, R. and Adler, J. (1995a). Effects of configurational, positional and vibrational degrees of freedom on an alloy phase diagram: a Monte Carlo study of $Ga_{1-x}In_xP$. J. Phys. Condens. Matter *7*, 1167.
Silverman, S. Zunger, A. Kalish, R. and Adler, J. (1995b). Atomic-scale of disordered $Ga_{1-x}In_xP$ alloys. Phys. Rev. B *51* 10795-10815.

Stobolov, S. V. and Cohen, R. E. (2002). First-principles calculations of the formation energy in MgO-CaO solid solutions. Phys. Rev. **B65** 092203-1

Tepesch, P. D. Kohan, A. F., Garbulsky, G. D., Ceder, G., Coley, C., Stokes, H. T., Boyer, L. L., Mehl, M. J. Burton, B. P., Kyeongjae, C. and Joannopoulos, (1996). J. Amer. Ceram. Soc. 79, 2033-2040.

Thompson, J.B. and Waldbaum, D.R. (1969). Analysis of the two-phase region halite-sylvite in the system NaCl-KCl. Geochimica et Cosmochimica Acta, **33**, 671-690.

van de Walle, A. and Asta, M. (2002). Self-driven lattice-model monte carlo simulations of alloy thermodynamic properties and phase diagrams. Modelling Simul. Mater. Sci. Eng., **10** p. 521.
van de Walle, A., Asta, M. and Ceder, G. (2002). The alloy theoretic automated toolkit: A

user guide. CALPHAD Journal **26** p. 539.
van de Walle, A., Ceder, G. and Waghmare, U.V. (1998). First-principles computation of the vibrational entropy of ordered and disordered Ni_3Al. Phys. Rev. Lett. **80**, 4911-4914.

van de Walle, A., and Ceder, G. (2000). First-principles computation of the vibrational entropy of ordered and disordered Pd_3V. Phys. Rev. **B61**, 5972-5978.

van de Walle A. and Ceder, G., (2002a). The effect of lattice vibrations on substitutional alloy thermodynamics. Rev. Mod. Phys. 74, 11.

van de Walle A. and Ceder, G., (2002b). Automating First-Principles Phase Diagram Calculations. Journal of Phase Equilibria, 23 p. 348.

Vanderbilt, D. 1990. Soft self-consistent pseudopotentials in a generalized eigenvalue formalism Phys. Rev. **B41**: 7892.
Walker D., Verma P. K., Cranswick L. M. D. Clark S. M., Jones R. L. and Bure S. (2005) Halitsylvite thermoconsolution Amer. Mineral. **90** 229-
Wolverton, C., and Ozolins, V. (2001). Entropically favored ordering: The metallurgy of Al_2Cu revisited. Phys. Rev. Lett. 86, p. 5518.

Wu, E., Ceder, G. and van de Walle, A. (2003). Using bond-length-dependent transferable force constants to predict vibrational entropies in Au-Cu, Au-Pd, and Cu-Pd alloys. Phys. Rev. **B67**, 134103-1-7.

TABLE I: Temperature Independent Effective Cluster Interactions in eV/mol.

Cluster Coordinates minus (0,0,0)	m(r,t) Multiplicity	ECI eV/cation
Zero Cluster	1	0.061742
Point Cluster	1	-0.001249
(1/2,0,1/2)	6	-0.004344
(1,0,0)	3	0.007531
(1/2,1,1/2)	12	-0.002448
(1,0,1)	6	0.000384
(1/2,0,3/2)	12	0.000243
(1,1,1)	4	-0.000825
(1/2,3/2,1)	24	-0.000836
(2,0,0)	3	0.000559
(2,1/2,1/2)	12	-0.000493
(0,3/2,3/2)	6	-0.000371
(1/2,0,-1/2), (0,-1/2,-1/2)	8	0.000515
(1/2,0,-1/2), (1,0,0)	12	-0.002659
(1/2,-1/2,0), (1/2,-1,1/2)	24	-0.000289
(0,-1,0), (1/2,-1,1/2)	24	0.000237
(1,-1/2,-1/2), (1/2,-1,1/2)	8	-0.001466
(1,-1/2,1/2), (1/2,-1,1/2)	24	0.000995
(1/2,-1,-1/2), (1/2,-1,1/2)	24	0.000675
(1/2,0,-1/2), (1,0,-1)	6	0.002104
(1,0,0), (1,0,-1)	12	-0.001100
(1/2,-1/2,0), (1/2,0,-1/2), (0,-1/2,-1/2)	2	-0.000883

TABLE II: End member molar volumes.

$System$	$V^{\dagger}_{EXP}$	V_{GGA}
$NaCl$	44.852	46.2
KCl	62.262	66.1

† Volumes are in $\mathring{A}^3/cation$. Experimental values are from Barrett and Wallace (1954).

FIGURE CAPTIONS

Figure 1) Comparison of 44 VASP ($\circ$) calculated formation energies, ΔE_f, and the cluster expansion fit ($\square$).

Figure 2) Nearest neighbor bond-stiffnesses (against bond-stretching or bond-bending) as functions of bond lengths. Diamonds and crosses indicate *ab initio* data points, and lines are linear fits used in the calculations of the vibrational free energy.

Figure 3) Calculated percentages of excess volumes for $Na_mK_nCl_{(m+n)}$ super-cells, $\bullet$; and experimental values calculated from data in Barrett and Wallace (1954). $V_{Vegard} = (1-X)V_{NaCl} + (X)V_{KCl}$, where X = mol fraction KCl.

Figure 4) Comparison of the calculated phase diagrams with experimental data that were tabulated in Thompson and Waldbaum (1969): the dashed curve is the phase diagram that was calculated without S_{VIB}; the solid curve was calculated with S_{VIB}; $\square$ = data of Nacken (1918); $\Diamond$ = data of Bunk and Tichelaar (1953); $\bigcirc$ =data of Barrett and Wallace (1954). $V_{Vegard} = (1-X)V_{NaCl} + (X)V_{KCl}$, where X = mol fraction KCl.

Figure 5) Nearest neighbor bond-stiffnesses as functions of composition in the NaCl-KCl (left) and MgO-CaO systems (right).

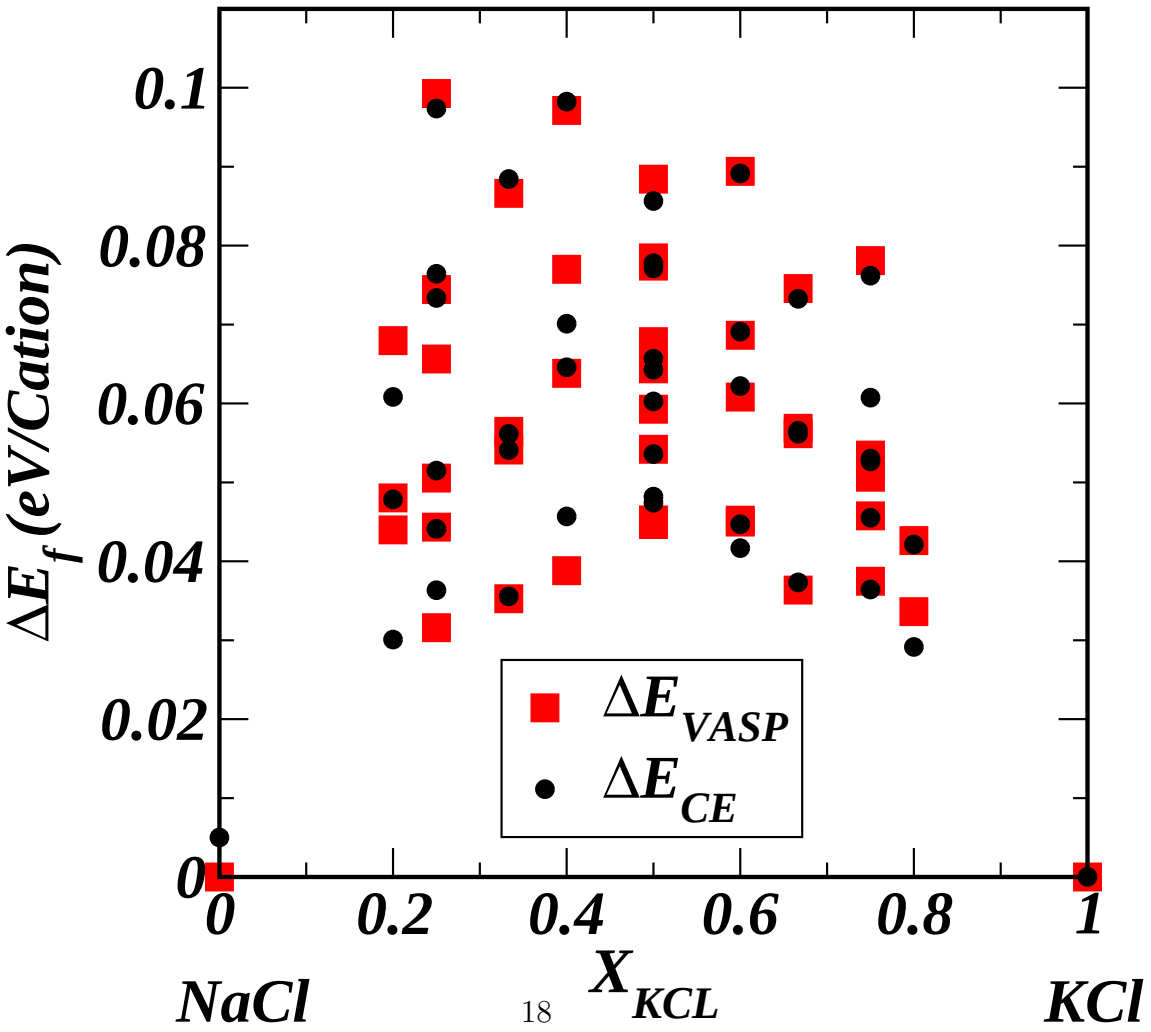
0.1
0.08
0.06
0.04
0.02
0
ΔE_f (eV/Cation)
ΔE_{VASP}
ΔE_{CE}
0
0.2
0.4
0.6
0.8
1
NaCl
X_{KCL}
KCl

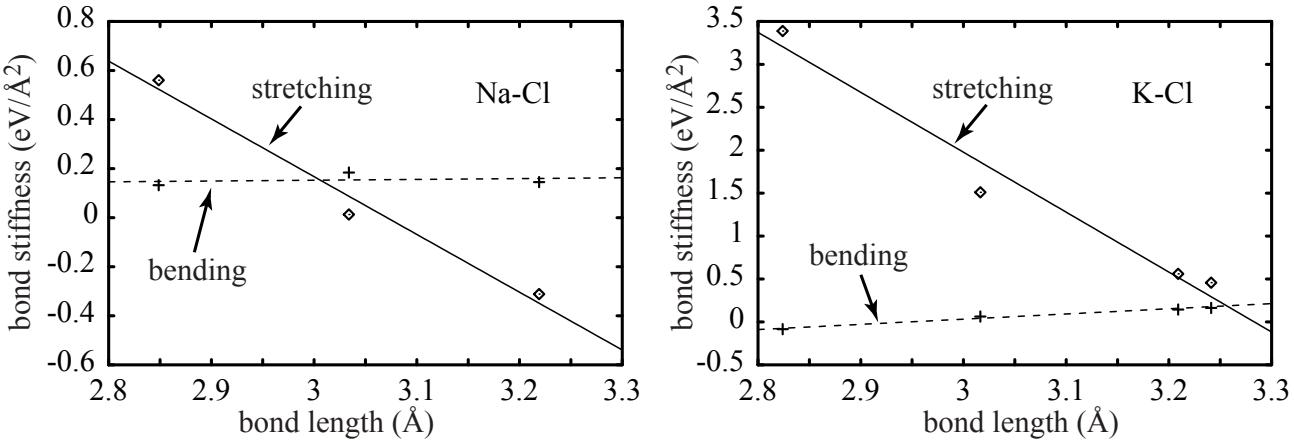

FIG. 2: Nearest neighbor bond-stiffnesses (against bond-stretching or bond-bending) as functions of bond lengths. Diamonds and crosses indicate *ab initio* data points, and lines are linear fits used in the calculations of the vibrational free energy.

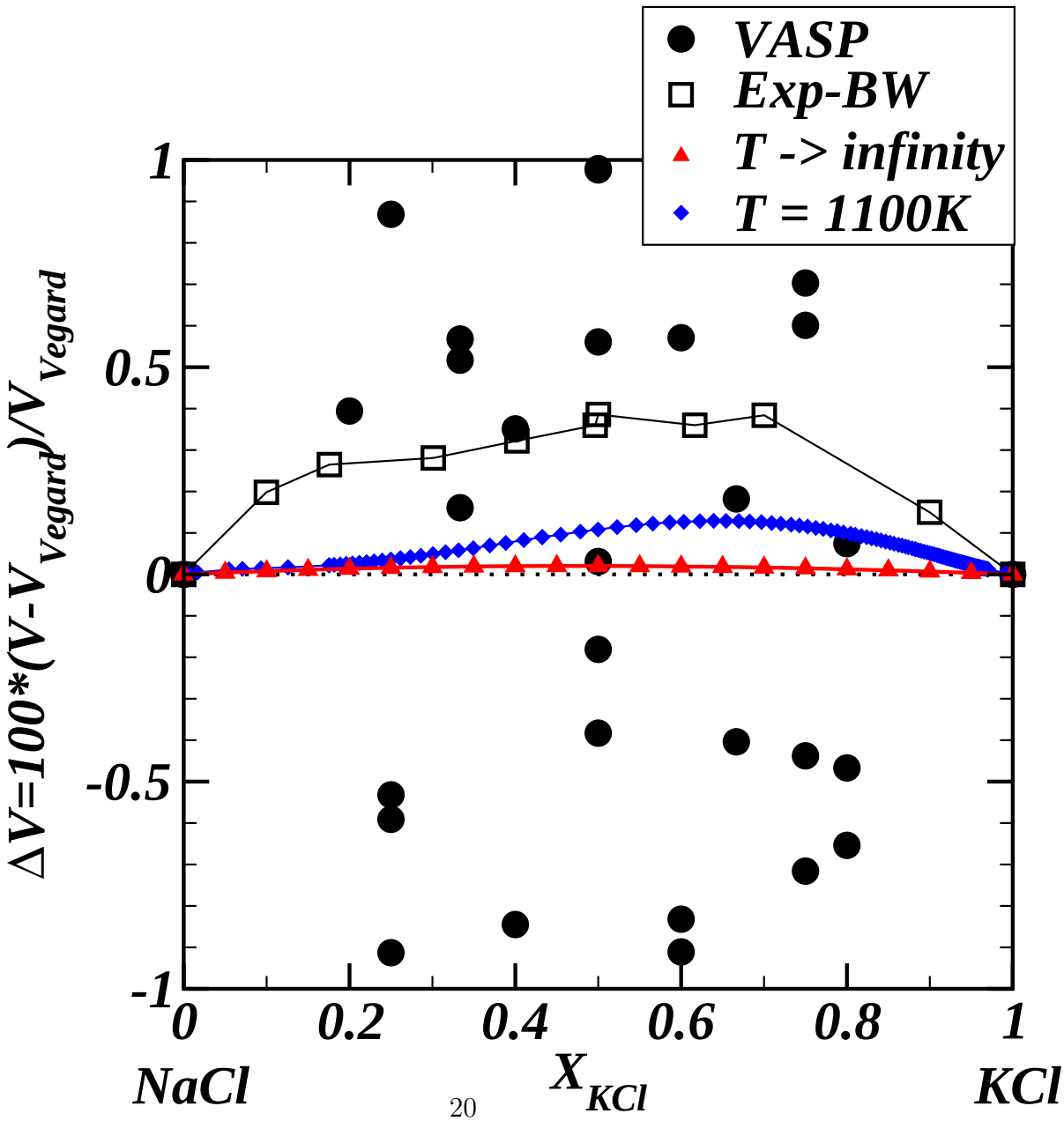
VASP
Exp-BW
T -> infinity
T = 1100K
1
0.5
0
-0.5
-1
0
0.2
0.4
0.6
0.8
1
NaCl
KCl
X_KCl
ΔV=100*(V-V_Vegard)/V_Vegard

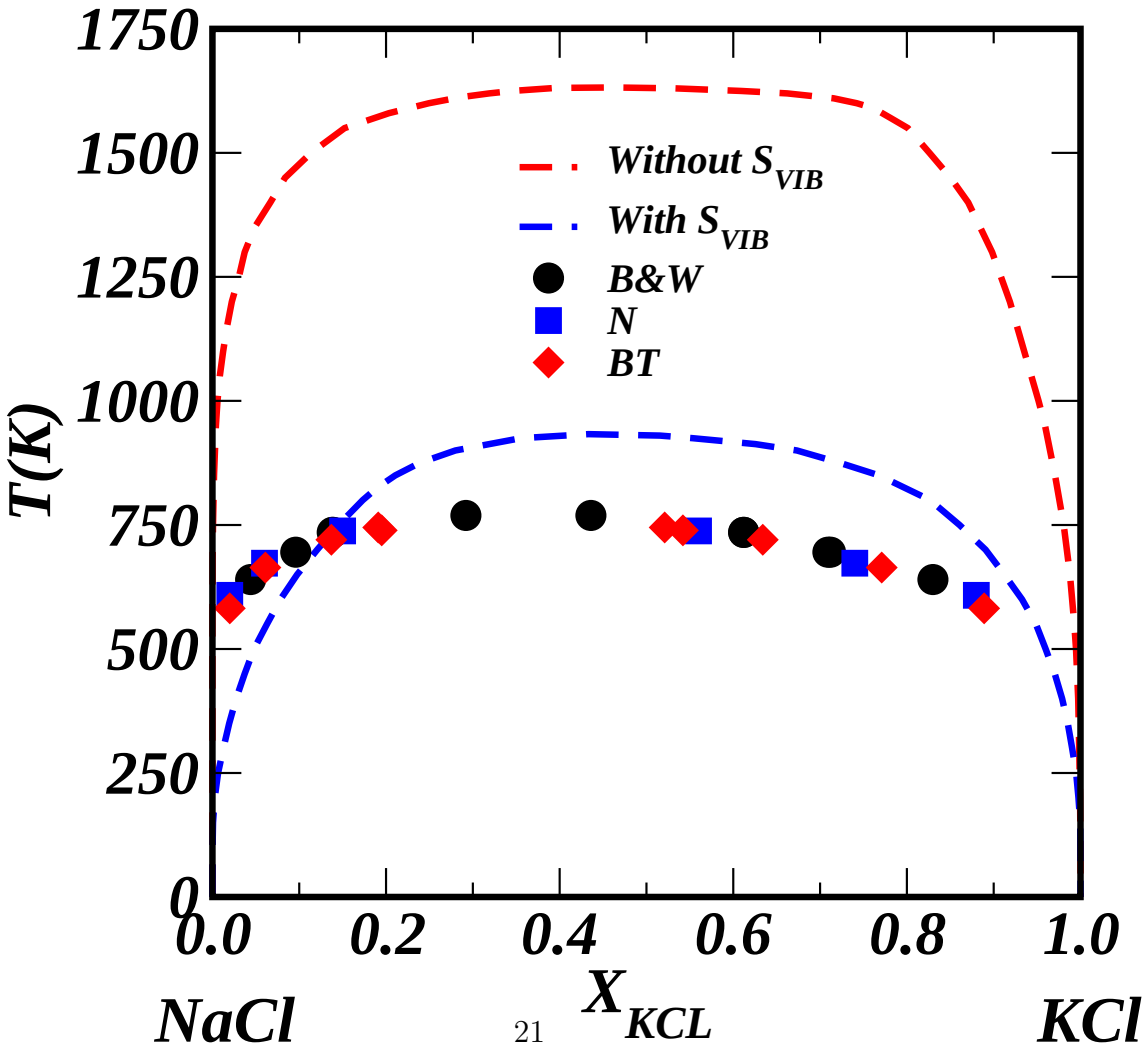
1750
1500
1250
1000
750
500
250
0
T(K)
Without S_{VIB}
With S_{VIB}
B&W
N
BT
0.0
0.2
0.4
0.6
0.8
1.0
NaCl
X_{KCL}
KCl

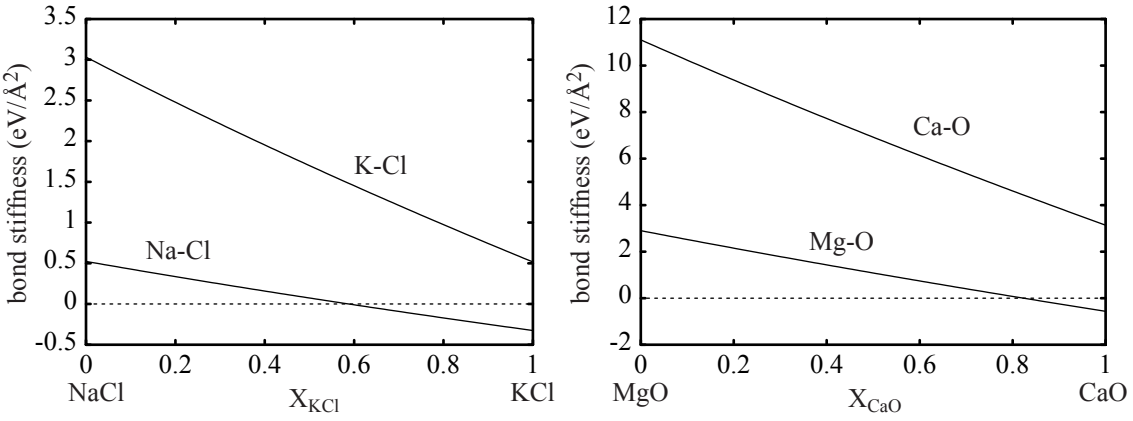

FIG. 5: Nearest neighbor bond-stiffnesses as functions of composition in the NaCl-KCl (left) and MgO-CaO systems (right).